Differential Modulation Diversity

R. Schober[1] and L.H.-J. Lampe[2]
[1]Department of Electr. & Comp. Engineering, University of Toronto
[2]Chair of Information Transmission, University of Erlangen-Nuremberg
rschober@comm.utoronto.ca, LLampe@LNT.de

Abstract— **In this paper, differential modulation diversity (DMD) is introduced. This diversity scheme is based on diagonal signal constellations which have been previously proposed for differential space–time modulation (DSTM). DMD can exploit both space and time diversity and DSTM, which is a pure space diversity scheme, results as a special case. A low–complexity noncoherent receiver originally designed for DSTM is adapted to DMD and the power efficiency of DMD for spatially correlated Rayleigh fading and imperfect interleaving is investigated.**

Keywords— **Differential modulation diversity, transmit diversity, space–time block codes, noncoherent detection.**

I. Introduction

RECENTLY , several coherent modulation schemes which can efficiently exploit the diversity of flat fading channels have been proposed. In [1], [2] fading resistant multi–dimensional signal constellations (space–time block codes) are introduced to make use of the diversity offered by multiple transmit antennas. Similarly, rotated one–dimensional [3] and multi–dimensional [4] signal constellations can be used for time diversity. In fact the space diversity schemes in [1], [2] and the time diversity scheme in [4] are closely related since in both cases a number of symbols is jointly modulated to obtain a multi–dimensional hypersymbol. Therefore, we refer to both techniques as *modulation diversity* [4]. Although for these coherent modulation schemes no channel state information (CSI) is required at the transmitter, perfect knowledge of the fading coefficients is necessary at the receiver. However, especially for fast fading channels it may be difficult or even impossible to obtain reliable channel estimates. Thus, differential space–time modulation (DSTM) schemes for multiple transmit antennas have been proposed by different authors [5], [6], [7]. DSTM allows noncoherent detection using e.g. conventional differential detection (DD), multiple–symbol detection (MSD), or decision–feedback differential detection (DF–DD) [8], i.e., explicit channel estimation is avoided.

DSTM exploits space diversity only. In [9] time diversity for M–ary differential phase shift keying (MDPSK) has been introduced by a repetition code which implies bandwidth expansion. MDPSK combined with a nonlinear block code has been proposed in [10]. Since in this scheme the diversity encoder and the differential encoder are separated by a symbol interleaver, only conventional DD can be applied while the application of more sophisticated techniques such as MSD or DF–DD is not possible.

Motivated by the above mentioned coherent modulation diversity schemes, we propose a *differential modulation diversity* (DMD) technique which is based on *diagonal signals* originally proposed for DSTM [5]. DMD can exploit both space and time diversity, and diagonal signals have the special advantage that noncoherent receivers [8] designed for DSTM can be employed after appropriate modifications.

It will be shown that for diagonal signals and fast fading a higher performance can be achieved if time diversity is exploited instead of space diversity. On the other hand, for slow fading and small delays (i.e., small interleaver lengths) space diversity is preferable. It will be also demonstrated that a combined approach, where both space and time diversity are exploited, enables a robust transmission scheme for a wide range of fading velocities.

II. Preliminaries

A. Notation

Bold upper case $\boldsymbol{X}$ and lower case $\boldsymbol{x}$ denote matrices and vectors, respectively. $\det(\cdot)$, $(\cdot)^T$, $(\cdot)^H$, and $(\cdot)^*$ refer to the determinant of a matrix, transposition, Hermitian transposition, and complex conjugation, respectively. $\mathrm{diag}\{x_1,\, x_2,\, \ldots,\, x_L\}$ is a diagonal matrix with main diagonal elements x_1, x_2, …, x_L, whereas $\boldsymbol{I}_M$ and $\boldsymbol{0}_M$ are the $M \times M$ identity matrix and the $M \times M$ all–zero matrix, respectively. $\Pr\{\cdot\}$, $\mathcal{E}\{\cdot\}$, $\otimes$, $j \triangleq \sqrt{-1}$, and $\Re\{\cdot\}$ denote the probability of the event in brackets, expectation, the Kronecker product, the imaginary unit, and the real part of a complex number, respectively. Throughout this paper, all signals are represented by their complex–baseband equivalents.

B. Rayleigh Fading Channel Model

We consider a transmission scheme using N_T transmit antennas and N_R receive antennas. We assume a flat Rayleigh fading channel, i.e., at time k the effect of fading between transmit antenna μ and receive antenna ν can be accounted for by the fading gain $h_{\mu\nu}[k]$ which is a zero–mean complex Gaussian random process. We presume that the fading gains of different antenna pairs may be mutually correlated but have the same statistical properties in the time direction. The space–time autocorrelation function (ACF) is denoted as

$$\varphi_{hh}[\lambda,\, \mu_1,\, \mu_2,\, \nu_1,\, \nu_2] \triangleq \mathcal{E}\{h_{\mu_1\nu_1}[k+\lambda]h^*_{\mu_2\nu_2}[k]\}, \qquad (1)$$

$0 \le \mu_1,\, \mu_2 \le N_T - 1$, $0 \le \nu_1,\, \nu_2 \le N_R - 1$. Although for the performance analysis in Section V the general model according to (1) is adopted, for the numerical results presented in Section VI we assume that the space–time ACF is separable into a spatial ACF $\varphi^s_{hh}[\mu_1,\, \mu_2,\, \nu_1,\, \nu_2]$ and a temporal ACF $\varphi^t_{hh}[\lambda]$

$$\varphi_{hh}[\lambda,\, \mu_1,\, \mu_2,\, \nu_1,\, \nu_2] = \varphi^s_{hh}[\mu_1,\, \mu_2,\, \nu_1,\, \nu_2] \cdot \varphi^t_{hh}[\lambda]. \qquad (2)$$

This useful simplification is frequently adopted in literature (cf. e.g. [11], [12]) and allows to investigate the influence of

temporal and spatial correlations on performance separately. Of course, due to the general form of (1) our analytical results also allow to evaluate receiver performance for physically more realistic models (cf. e.g. [13]).

Here, for the temporal ACF Clarke's model [14] is adopted

$$\varphi_{hh}^{t}[\lambda] = \sigma_h^2 \cdot \mathrm{J}_0(2\pi B_f T \lambda), \tag{3}$$

where $\mathrm{J}_0(\cdot)$ is the zeroth order Bessel function of the first kind and σ_h^2, B_f, and T denote the variance of the fading process, the single–sided bandwidth of the underlying continuous–time fading process, and the symbol duration, respectively.

For the spatial ACF function the same simple model as in [11] is used

$$\varphi_{hh}^{s}[\mu_1, \mu_2, \nu_1, \nu_2] \quad = \quad \begin{cases} 1 & \text{if } \mu_1 = \mu_2,\ \nu_1 = \nu_2 \\ \rho & \text{otherwise} \end{cases} \tag{4}$$

where ρ, $0 \le \rho \le 1$, refers to the space–correlation coefficient. Note that for our numerical results we restrict the application of this model with $\rho > 0$ to the case $N_T \le 3$ and $N_R = 1$ since otherwise it would be rather unrealistic.

Furthermore, the discrete–time received signal at antenna ν is impaired by a complex additive white Gaussian noise (AWGN) process $n_\nu[k]$.The AWGN processes at different receive antennas are assumed to be mutually independent and have equal variance $\sigma_n^2 = \mathcal{E}\{|n_\nu[k]|^2\}$, $0 \le \nu \le N_R - 1$.

C. Diagonal Signals

For the proposed DMD scheme, diagonal signals [5], [6] are used which may be considered as a multi–dimensional generalization of MDPSK modulation. The diagonal matrix $\boldsymbol{S}[k] = \mathrm{diag}\{s_0[k], s_1[k], \ldots, s_{N_S-1}[k]\}$ of N_S jointly modulated transmitted symbols $s_\eta[k]$, $0 \le \eta \le N_S - 1$, is obtained by differential encoding from $\boldsymbol{S}[k-1]$ and the matrix $\boldsymbol{V}[k]$ of (differential) information symbols

$$\boldsymbol{S}[k] = \boldsymbol{V}[k]\boldsymbol{S}[k-1]. \tag{5}$$

$\boldsymbol{V}[k] = \boldsymbol{V}_{l[k]} = (\boldsymbol{V}_1)^{l[k]}$ is taken from the set $\mathcal{A} = \{\boldsymbol{V}_l = \mathrm{diag}\{\exp(j2\pi u_0 l/L), \exp(j2\pi u_1 l/L), \ldots, \exp(j2\pi u_{N_S-1} l/L)\} | l \in \{0, 1 \ldots, L-1\}\}$. We observe that matrix $\boldsymbol{V}[k]$ is uniquely associated with symbol $l[k]$. The alphabet size L is given by $L = 2^{N_S R}$ where R denotes the data rate in bits per channel use. For optimum power efficiency, the coefficients u_η, $0 \le \eta \le N_S - 1$, have to be optimized to maximize the diversity product [5]. For the numerical results presented in Section VI, the parameters given in [5, Table I] are adopted. In order to minimize BER for a given symbol error rate, $N_S R$ bits should be assigned via Gray labeling to the symbols l. As outlined in [8], a Gray labeling can be found for all constellations given in [5, Table I], but for the constellation $N_S = 4$, $R = 1\,\mathrm{bit/(channel\,use)}$ where a natural labeling may be used.

III. Differential Modulation Diversity

In this section, different forms of DMD are discussed. First, space diversity is briefly reviewed. Then it is shown how time diversity can be introduced and finally a generalization of both approaches is given.

A. Space Diversity

In [5] it is proposed that all non–zero elements of matrix $\boldsymbol{S}[k]$ are transmitted over different antennas, i.e., $N_S = N_T$ is valid and at time $N_T k + \mu$, $0 \le \mu \le N_T - 1$, $s_\mu[k]$ is transmitted over antenna μ whereas no symbol is transmitted over the remaining antennas. Hence, the received signal at time $N_T k + \mu$ at receive antenna ν is

$$r_\nu[N_T k + \mu] = h_{\mu\nu}[N_T k + \mu] s_\mu[k] + n_\nu[N_T k + \mu]. \tag{6}$$

For this diversity scheme (referred to as DSTM in [5]) $N_T > 1$ transmit antennas are required to obtain a diversity gain if only one receive antenna is available. On the other hand, the delay of this scheme is very low (N_T modulation intervals) since no interleaver is necessary to achieve diversity. Furthermore, the scheme can also provide a diversity gain for time–invariant channels. However, each transmit antenna is active only every $N_T$ths symbol interval, i.e., the *effective* fading bandwidth relevant for the receiver is $N_T B_f T$ instead of $B_f T$. This has a negative influence on receiver performance (e.g. the error floor for conventional DD increases with increasing fading bandwidth [8]).

B. Time Diversity

Here, N_B symbols are jointly modulated as described in Section II-C and transmitted over one antenna, i.e., $N_B = N_S$, $N_T = 1$. More specifically, to achieve diversity a block of $N_B N_I$ symbols $s_\kappa[k]$, $0 \le \kappa \le N_B - 1$, $0 \le k \le N_I - 1$, is built, and interleaved by an $N_I \times N_B$ rectangular interleaver (cf. Fig. 1) and the resulting stream of symbols is transmitted. At the output of a corresponding de–interleaver the received signal at time $N_B k + \kappa$, at receive antenna ν is

$$r_\nu[N_B k + \kappa] = h_{0\nu}[N_I \kappa + k] s_\kappa[k] + n_\nu[N_I \kappa + k], \tag{7}$$

$0 \le \kappa \le N_B - 1$, $0 \le k \le N_I - 1$. Since the transmit antenna is active in each symbol interval, the effective fading bandwidth is $B_f T$ independent of N_B. On the other hand, no diversity gain can be realized if the channel is time–invariant, and a transmission delay of $N_B N_I$ is introduced. In particular, for given k and ν the fading gains $h_{0\nu}[N_I \kappa + k]$, $0 \le \kappa \le N_B - 1$, should be approximately uncorrelated to ensure full diversity for the jointly modulated symbols $s_\kappa[k]$, $0 \le \kappa \le N_B - 1$.

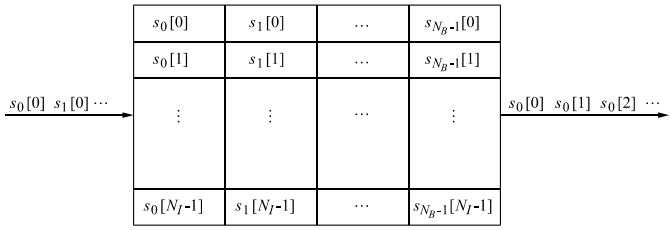

Fig. 1. $N_I \times N_B$ rectangular interleaver.

C. Space and Time Diversity

In order to exploit both space and time diversity, $N_S = N_B N_T$ symbols are jointly modulated (cf. Section II-C). Then a block $\boldsymbol{s}$=[$s_0[0]$ $s_1[0]$ $\ldots$ $s_{N_T N_B-1}[0]$ $s_0[1]$ $\ldots$ $s_{N_T N_B-1}[N_I-$

1]] of $N_T N_B N_I$ symbols is built (cf. Fig. 2a)) and partitioned into N_T subblocks $\boldsymbol{s}_\mu$=[$s_\mu[0]$ $s_{N_T+\mu}[0]$ ... $s_{N_T(N_B-1)+\mu}[0]$ $s_\mu[1]$ ... $s_{N_T(N_B-1)+\mu}[N_I-1]$], $0 \le \mu \le N_T-1$, of length $N_B N_I$ by serial/parallel (S/P) conversion. Each of these subblocks is associated with one transmit antenna and interleaved by an $N_I \times N_B$ rectangular interleaver Π. At time $N_T N_I \kappa + N_T k + \mu$, $0 \le \mu \le N_T-1$, $0 \le \kappa \le N_B-1$, $0 \le k \le N_I-1$, antenna μ transmits the symbol $s_{N_T\kappa+\mu}[k]$, while the remaining N_T-1 antennas are not active.

At receive antenna ν the sampled received signal is collected in a block $\tilde{\boldsymbol{r}}_\nu$=[$\tilde{r}_\nu[0]$ $\tilde{r}_\nu[1]$ ... $\tilde{r}_\nu[N_T N_B N_I-1]$] of length $N_T N_B N_I$ (cf. Fig. 2b)). This block is serial/parallel converted into N_T subblocks $\tilde{\boldsymbol{r}}_\nu^\mu$=[$\tilde{r}_\nu[\mu]$ $\tilde{r}_\nu[N_T+\mu]$ ... $\tilde{r}_\nu[N_T(N_B N_I-1)+\mu]$], $0 \le \mu \le N_T-1$, of length $N_B N_I$. Each of these subblocks is de–interleaved with the inverse of Π and the resulting subblocks are parallel/serial converted to obtain the block $\boldsymbol{r}_\nu$=[$r_\nu[0]$ $r_\nu[1]$ ... $r_\nu[N_T N_B N_I-1]$] of length $N_T N_B N_I$. Here, N_T de–interleavers Π^{-1} per receive antenna are required. Nevertheless, a modified de–interleaver $\tilde{\Pi}^{-1}$ can be employed which directly maps $\tilde{\boldsymbol{r}}_\nu$ to $\boldsymbol{r}_\nu$, of course.

The received signal at time $N_T N_B k + N_T \kappa + \mu$ at receive antenna ν is given by

$$r_\nu[N_T N_B k + N_T \kappa + \mu] = h_{\mu\nu}[N_T N_I \kappa + N_T k + \mu] \cdot s_{N_T\kappa+\mu}[k] + n_\nu[N_T N_I \kappa + N_T k + \mu], \quad (8)$$

$0 \le \mu \le N_T-1$, $0 \le \kappa \le N_B-1$, $0 \le k \le N_I-1$. This approach is a generalization of the schemes of Sections III-A and III-B which result as special cases for $N_B = 1$ ($N_I = 0$) and $N_T = 1$, respectively. Here, the delay is $N_T N_B N_I$ modulation intervals. The effective fading bandwidth relevant for the receiver is $N_T B_f T$.

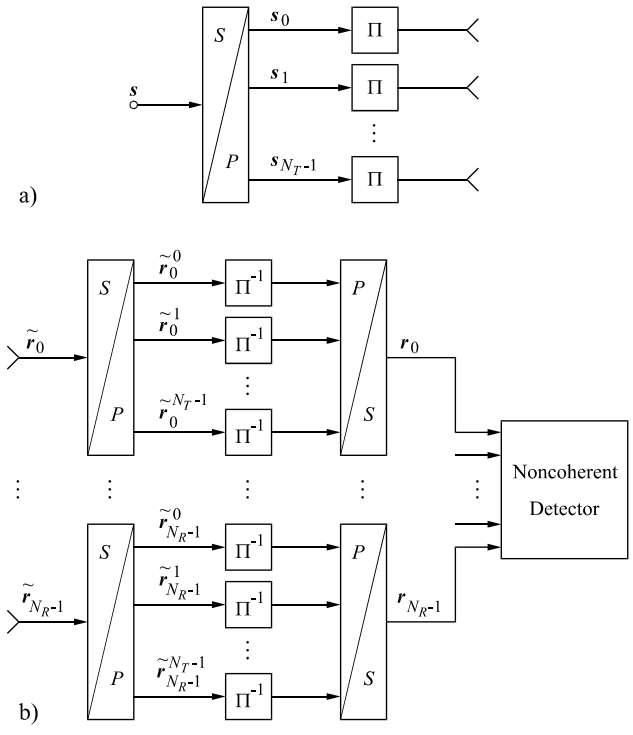

Fig. 2. Simplified block diagram for DMD: a) transmitter and b) receiver.

IV. Decision–Feedback Differential Detection

The general DMD scheme of Section III-C will be adopted in the following and specialized if necessary. For receiver design perfect interleaving and zero spatial correlation are presumed. The effect of imperfect interleaving and non–zero spatial correlation on the performance of the proposed receiver is investigated in Section VI. Since DSTM may be viewed as a special case of this general approach, it is possible to adapt receivers for DSTM [5], [8] to the problem at hand. In particular, we employ DF–DD since this schemes offers a similar performance as MSD while its complexity is comparable to that of conventional DD. Modifying the DF–DD scheme proposed in [8], we obtain the decision rule [15]

$$\hat{l}[k] = \underset{l}{\operatorname{argmax}} \left\{ \Re\left\{ \sum_{\mu=0}^{N_T-1} \sum_{\kappa=0}^{N_B-1} \sum_{\nu=0}^{N_R-1} \exp\left(j\frac{2\pi u_{N_T\kappa+\mu} l}{L}\right) r_\nu^*[N_T N_B k + N_T \kappa + \mu] \cdot \hat{r}_{\mathrm{ref},\nu}[N_T N_B (k-1) + N_T \kappa + \mu] \right\} \right\}, \quad (9)$$

where $\hat{l}[k]$ denotes the estimated symbol and the reference symbol is given by

$$\hat{r}_{\mathrm{ref},\nu}[N_T N_B (k-1) + N_T \kappa + \mu] = \sum_{\xi=1}^{N-1} p_\xi \prod_{m=1}^{\xi-1} \exp\left(j\frac{2\pi u_{N_T\kappa+\mu} \hat{l}[k-m]}{L}\right) \cdot r_\nu[N_T N_B (k-\xi) + N_T \kappa + \mu]. \quad (10)$$

Here, p_ξ, $1 \le \xi \le N-1$, are the coefficients of an $(N-1)$st order linear predictor for the process

$$c_{\mu\nu}[N_T k] \triangleq h_{\mu\nu}[N_T k] + n_\nu[N_T k], \quad (11)$$

$0 \le \mu \le N_T-1$, $0 \le \nu \le N_R-1$. The predictor coefficients can be calculated from the *Wiener–Hopf equation* [16] or adaptively by application of the recursive least–squares (RLS) algorithm [17], [18], [8]. Note that DF–DD with $N = 2$ is equivalent to conventional DD. For the DF–DD decision rule according to (9) $2^{N_T N_B R}/(N_T N_B R)$ metrics per bit decision have to be calculated, i.e., the same number as for conventional DD [5].

V. Performance Analysis

In this section, the performance of DMD with DF–DD is analyzed for spatially correlated Rayleigh fading and imperfect interleaving. Also the special cases of independent diversity branches and infinite observation window ($N \to \infty$) will be briefly discussed. Since it is difficult to take into account the effect of error propagation, for our analysis we assume perfect feedback for calculation of the reference signal as it is customary in literature [19], [18], i.e., $l[k-m]$ is used in (10) instead of $\hat{l}[k-m]$, $1 \le m \le N-1$.

A. Pairwise Error Probability

The pairwise error probability $P_e(l_1, l_2)$ is the probability of detecting $\hat{l}[k] = l_2$, when $l[k] = l_1$ ($l_1, l_2 \in \{0, 1, \ldots, L-1\}$, $l_1 \neq l_2$) is transmitted.

A.1 General Case

Using (8), (9), and (10) it is straightforward to show that $P_e(l_1, l_2)$ can be expressed as [15]

$$P_e(l_1, l_2) = \Pr\{\Delta(l_1, l_2) < 0\}, \tag{12}$$

where $\Delta(l_1, l_2)$ is defined as

$$\Delta(l_1, l_2) \triangleq \sum_{\mu=0}^{N_T-1} \sum_{\kappa=0}^{N_B-1} \sum_{\nu=0}^{N_R-1} (C_{\mu\kappa} x_{\mu\nu}[k, \kappa] y^*_{\mu\nu}[k-1, \kappa] + C^*_{\mu\kappa} x^*_{\mu\nu}[k, \kappa] y_{\mu\nu}[k-1, \kappa]) \tag{13}$$

with

$$C_{\mu\kappa} \triangleq 1 - \exp\left(j 2\pi u_{N_T\kappa+\mu}(l_1 - l_2)/L\right) \tag{14}$$

$$x_{\mu\nu}[k, \kappa] \triangleq h_{\mu\nu}[N_T N_I \kappa + N_T k + \mu] + n_\nu[N_T N_I \kappa + N_T k + \mu] s^*_{N_T\kappa+\mu}[k] \tag{15}$$

$$y_{\mu\nu}[k-1, \kappa] \triangleq \sum_{\xi=1}^{N-1} p_\xi x_{\mu\nu}[k-\xi, \kappa]. \tag{16}$$

Using vector notation, $\Delta(l_1, l_2)$ can be rewritten as

$$\Delta(l_1, l_2) = \boldsymbol{g}^H \boldsymbol{F} \boldsymbol{g} \tag{17}$$

with

$$\boldsymbol{g} \triangleq [\boldsymbol{x}^T \ \boldsymbol{y}^T]^T \tag{18}$$

$$\boldsymbol{F} \triangleq \begin{bmatrix} \boldsymbol{0}_{N_T N_B N_R} & \boldsymbol{C}^H \\ \boldsymbol{C} & \boldsymbol{0}_{N_T N_B N_R} \end{bmatrix} \tag{19}$$

$$\boldsymbol{x} \triangleq [x_{00}[k, 0] \ \ldots \ x_{N_T-1\,0}[k, 0] \ x_{00}[k, 1] \ \ldots \ x_{N_T-1\,N_R-1}[k, N_B-1]]^T \tag{20}$$

$$\boldsymbol{y} \triangleq [y_{00}[k-1, 0] \ \ldots \ y_{N_T-1\,0}[k-1, 0] \ y_{00}[k-1, 1] \ \ldots \ y_{N_T-1\,N_R-1}[k-1, N_B-1]]^T \tag{21}$$

$$\boldsymbol{C} \triangleq \boldsymbol{I}_{N_R} \otimes \operatorname{diag}\{C_{00}, C_{10}, \ldots, C_{N_T-1\,N_B-1}\}. \tag{22}$$

The two–sided Laplace transform of the probability density function (pdf) $p_{\Delta(l_1,l_2)}(x)$ of $\Delta(l_1, l_2)$ can be expressed as [20]

$$\Phi_{\Delta(l_1,l_2)}(s) = \int_{-\infty}^{\infty} p_{\Delta(l_1,l_2)}(x) e^{-sx} \, \mathrm{d}x = \frac{1}{\det(\boldsymbol{I}_{2N_T N_B N_R} + s\boldsymbol{\Phi}_{gg}\boldsymbol{F})} \tag{23}$$

where the definition $\boldsymbol{\Phi}_{gg} \triangleq \mathcal{E}\{\boldsymbol{g}\boldsymbol{g}^H\}$ is used. $P_e(l_1, l_2)$ can be calculated directly from $\Phi_{\Delta(l_1,l_2)}(s)$ [20]

$$P_e(l_1, l_2) = \frac{1}{2\pi j} \int_{\gamma-j\infty}^{\gamma+j\infty} \Phi_{\Delta(l_1,l_2)}(s) \frac{\mathrm{d}s}{s} \tag{24}$$

for $0 < \gamma < \Re\{s_1\}$, where s_1 refers to that pole of $\Phi_{\Delta(l_1,l_2)}(s)$ which has minimum positive real part. A closed form solution for the integral in (24) may be obtained using the residue method proposed in [21]. However, in practice it may be quite cumbersome to determine the residues. Therefore, the numerical results in Section VI are obtained using a technique reported in [22] which is based on Gauss–Chebyshev quadrature rules and can be straightforwardly applied to (24) [15].

It is worth mentioning that the pairwise error probability for coherent reception with perfect CSI can also be obtained from the above results if $\boldsymbol{y} \triangleq [h_{00}[N_T k] \ \ldots \ h_{N_T-1\,N_R-1}[N_T k + N_T N_I (N_B - 1) + N_T - 1]]^T$ is adopted (i.e., $\boldsymbol{y}$ is identical with $\boldsymbol{x}$ for $\sigma_n^2 = 0$).

A.2 Independent Diversity Branches

In order to get more intuitive insight, we simplify the general results of the previous section to the important special case where all diversity branches are mutually uncorrelated (i.e., no spatial correlation and perfect interleaving). Using similar methods as in [23, Appendix B] and [24], [8], it can be shown that $P_e(l_1, l_2)$ may be expressed as

$$P_e(l_1, l_2) = \frac{1}{\pi} \int_0^{\pi/2} \prod_{\mu=0}^{N_T-1} \prod_{\kappa=0}^{N_B-1} \left(\frac{1}{1 + \frac{\alpha_{\mu\kappa}(l_1,l_2)}{4\cos^2\Theta}} \right)^{N_R} \mathrm{d}\Theta, \tag{25}$$

where the definitions

$$\alpha_{\mu\kappa}(l_1, l_2) \triangleq 4 \frac{\sigma_h^2 + \sigma_n^2 - \sigma_e^2}{\sigma_e^2} \left(1 - d^2_{\mu\kappa}(l_1, l_2)\right) \tag{26}$$

$$d_{\mu\kappa}(l_1, l_2)) \triangleq |\cos(\pi u_{N_T\kappa+\mu}(l_1 - l_2)/L)| \tag{27}$$

are used and $\sigma_e^2 = \sigma_h^2 + \sigma_n^2 - \sum_{\xi=1}^{N-1} p_\xi^* \varphi^t_{hh}[N_T \xi]$ is the prediction error variance of the $(N-1)$st order linear predictor for process $c_{\mu\nu}[N_T k]$ (cf. (11)). Eq. (25) only requires the evaluation of an one–dimensional integral over a finite support which can be done easily by numerical integration.

From (25) the Chernoff upper bound [23, Appendix B]

$$P_e(l_1, l_2) \leq \frac{1}{2} \prod_{\mu=0}^{N_T-1} \prod_{\kappa=0}^{N_B-1} \left(\frac{1}{1 + \frac{\alpha_{\mu\kappa}(l_1,l_2)}{4}} \right)^{N_R} \tag{28}$$

is easily obtained. Eqs. (26) and (28) clearly show that $P_e(l_1, l_2)$ decreases with decreasing prediction error variance σ_e^2. Since σ_e^2 increases with increasing (effective) fading bandwidth $N_T B_f T$ [24], it can be concluded that for sufficient interleaving exploiting time diversity (i.e., increasing N_B) is more rewarding than exploiting space diversity (i.e., increasing N_T).

The limiting performance of DF–DD can be achieved for $N \to \infty$. Using the results of [18] (the fading ACF given in (3) is assumed), and taking into account that the effective fading bandwidth is $N_T B_f T$, we are able to shown that the minimum prediction error variance $\sigma^2_{e,\min}$ can be expressed as

$$\sigma^2_{e,\min} = \sigma_n^2 \left(\frac{\mathrm{e}\, \sigma_h^2}{2\pi N_T B_f T \sigma_n^2} \right)^{2N_T B_f T} \exp(2 N_T B_f T C_0) \tag{29}$$

(e is the Euler number) with

$$C_0 = \int_0^{\pi/2} \log\left(1 + \frac{\pi N_T B_f T \sigma_n^2}{\sigma_h^2} \sin\varphi\right) \sin\varphi \mathrm{d}\varphi. \qquad (30)$$

Eqs. (25)–(27) and (29), (30) will be used in Section VI to investigate the limiting performance of DMD with DF–DD for uncorrelated diversity branches.

For coherent reception with perfect CSI and independent Rayleigh fading diversity branches the pairwise error probability is obtained by replacing σ_e^2 by σ_n^2 in (26), i.e., for $\sigma_e^2 = \sigma_n^2$ (25) and (28) give the pairwise error probability and a corresponding Chernoff upper bound.

Note that $\sigma_{e,\min}^2 = \sigma_n^2$ also results for DF–DD with $N \to \infty$ if $B_f T \to 0$ is true (cf. e.g. (29)), i.e., in this case the performance of a coherent receiver can be approached. However, for $B_f T > 0$, $\sigma_{e,\min}^2 > \sigma_n^2$ holds even for $N \to \infty$ and a loss in performance is inevitable.

B. Approximation for BER

The results of the previous section may be used to obtain an approximation for BER. If we take into account that the matrices $\boldsymbol{V}_l$, $0 \le l \le L-1$, form a group under matrix multiplication [5], approximate the symbol error rate by the union bound, and assume that a Gray labeling for the $N_T N_B R$ bits assigned to the symbols l (i.e., matrix $\boldsymbol{V}_l$), $0 \le l \le L-1$, exists, a simple approximation for the BER for genie–aided DF–DD is given by

$$P_b^{\text{genie}} \approx \frac{1}{N_T N_B R} \sum_{l=1}^{L-1} P_e(l, 0). \qquad (31)$$

In general, for $N > 2$ erroneous feedback symbols increase BER approximately by a factor of two (cf. [19], [18], [8]). Hence, an approximation for the BER of realizable DF–DD is

$$P_b \approx \begin{cases} P_b^{\text{genie}}, & N = 2 \\ 2 \cdot P_b^{\text{genie}}, & N > 2 \end{cases}. \qquad (32)$$

VI. Results and Discussion

In this section, we restrict ourselves to the case of one receive antenna ($N_R = 1$), since the main focus of this work is on transmit (modulation) diversity. For the following, we define the signal–to–noise ratio (SNR) as $\mathrm{SNR} \triangleq \sigma_h^2/\sigma_n^2$. For the numerical approximation of BER the results of the previous section are used.

First, we consider DMD with time diversity, i.e., one transmit antenna is used ($N_T = 1$). Figs. 3a), b), and c) show BER vs. SNR for $N_B = 1$, $N_B = 2$, and $N_B = 3$, respectively. $R = 1\,\text{bit}/(\text{channel use})$ and $B_f T = 0.03$ are adopted. In addition, the interleaver length is $N_I = 1000$, i.e., the diversity branches can be considered as uncorrelated. It can be observed that significant performance gains are achieved by increasing N_B. In addition, DF–DD with $N > 2$ yields a higher power efficiency than conventional DD ($N = 2$) and in the SNR range of interest an error floor can be avoided. For comparison also asymptotic results for $N \to \infty$ are shown. We note that the numerical approximation and the simulation results match remarkably well.

In Fig. 4 (only numerical results are shown) we restrict the delay to $N_T N_B N_I \le 400$ modulation intervals in order to enable a fair comparison between DMD with space and time diversity. Zero spatial correlation is assumed ($\rho = 0$). $N_T N_B = 4$ and $R = 2\,\text{bits}/(\text{channel use})$ are adopted. For $B_f T = 0.001$ (Fig. 4a)), in general, the pure space diversity scheme ($N_T = 4$, $N_B = 1$) yields the best performance. The combined approach ($N_T = 2$, $N_B = 2$) performs similarly well. For $N = 2$ and high SNRs it performs even better because the effective fading bandwidth $N_T B_f T$ is smaller. The pure time diversity scheme ($N_T = 1$, $N_B = 4$) suffers from the relatively strong correlations between the different diversity branches due to imperfect interleaving. For $B_f T = 0.01$ (Fig. 4b)) the pure time diversity scheme offers the best performance. The space diversity scheme suffers from the larger effective fading bandwidth, whereas for $N = 5$ the loss for the combined approach is relatively small. For coherent reception all approaches yield almost the same BER, i.e., the interleaver length is large enough to guarantee independent diversity branches also for pure time diversity. From Fig. 4 it can be concluded that the combined approach ($N_T = 2$, $N_B = 2$) is more robust against variations of the fading bandwidth than pure space or time diversity schemes.

In Figs. 5a) and b) the influence of antenna correlation is investigated for $N_T = 2$ and $N_T = 3$, respectively. For comparison in both figures also the numerical results for $N_T = 1$ are shown. $N_B = 1$, $R = 1\,\text{bit}/(\text{channel use})$, and $B_f T = 0.02$ are valid. For spatial correlation the model according to (4) is adopted. Obviously, DMD is quite robust against spatial correlations. For a correlation factor of $\rho = 0.5$ the loss compared to uncorrelated diversity branches ($\rho = 0$) is very small. Even for strong correlations ($\rho = 0.9$) DMD with $N_T = 2$ and $N_T = 3$ outperforms the scheme without diversity ($N_T = 1$) if DF–DD with $N = 5$ or coherent detection are employed. For $\rho = 0.9$ and DF–DD with $N = 2$, $N_T = 1$ yields the best performance because of the smaller effective fading bandwidth. It is worth mentioning that simulation and numerical results show a good agreement.

VII. Conclusions

In this paper, DMD based on diagonal signals has been introduced. DMD can exploit both space and time diversity, i.e., DSTM which exploits space diversity only can be considered as a special case. The pairwise error probability for DMD with DF–DD has been derived for Rayleigh fading with spatial correlations and imperfect interleaving. This error analysis clearly shows that, in contrast to time diversity, space diversity increases the effective fading bandwidth which has a negative influence on receiver performance. It has been shown that a robust modulation scheme with high performance for a wide range of fading velocities results if space and time diversity are combined. Further investigations have shown that DMD also yields a significant performance gain for Ricean fading with moderately large line–of–sight component [15].

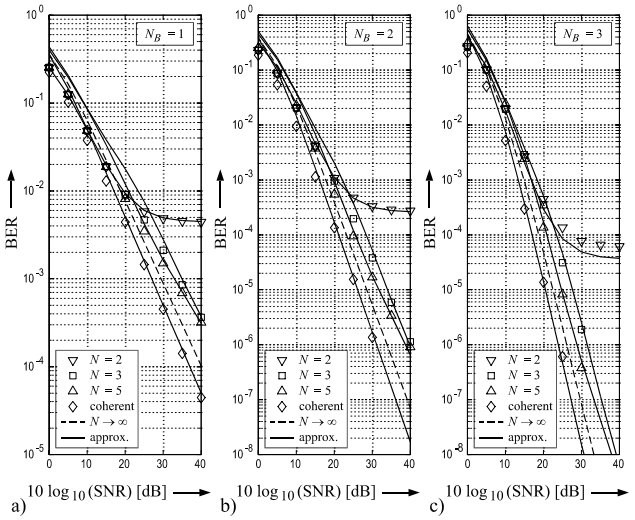

Fig. 3. BER vs. $10\log_{10}(\mathrm{SNR})$ for DF–DD with a) $N_B = 1$, b) $N_B = 2$, and c) $N_B = 3$ and Rayleigh fading. $\bigtriangledown$, $\square$, $\bigtriangleup$, and $\diamond$ denote simulation points.

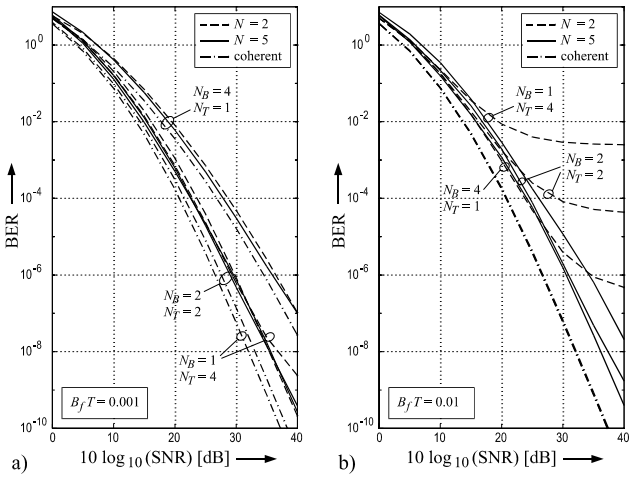

Fig. 4. BER vs. $10\log_{10}(\mathrm{SNR})$ for Rayleigh fading with a) $B_f T = 0.001$ and b) $B_f T = 0.01$. Numerical results are shown.

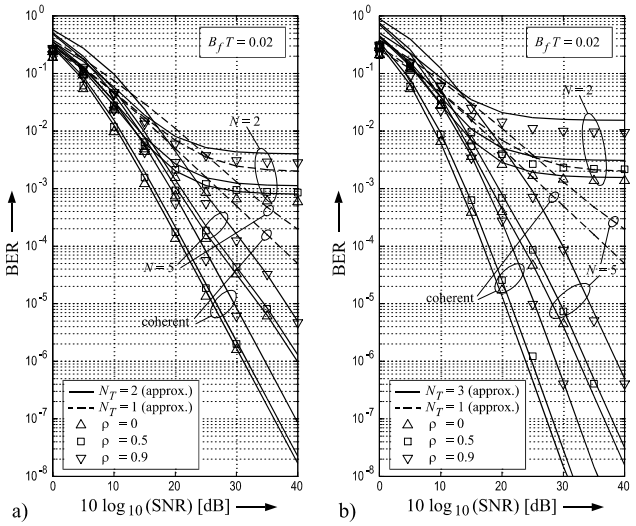

Fig. 5. BER vs. $10\log_{10}(\mathrm{SNR})$ for Rayleigh fading with spatial correlations and a) $N_T = 2$ and b) $N_T = 3$. $\bigtriangledown$, $\square$, and $\bigtriangleup$ denote simulation points.

REFERENCES

[1] V.M. DaSilva and E.S. Sousa, "Fading–Resistant Modulation Using Several Transmitter Antennas," *IEEE Trans. on Commun.*, vol. COM-45, pp. 1236–1244, Oct. 1997.

[2] S.M. Alamouti, "A Simple Transmitter Diversity Scheme for Wireless Communications," *IEEE Journal on Selected Areas in Communications*, vol. SAC-16, pp. 1451–1458, Oct. 1998.

[3] K. Boulle and J.C. Belfiore, "Modulation Scheme Designed for Flat Fading and AWGN Cannels," in *Proccedings of CISS'92*, Princeton, Mar. 1992.

[4] J. Boutros and E. Viterbo, "Signal Space Diversity: A Power- and Bandwidth–Efficient Diversity Technique for the Rayeigh Fading Channel," *IEEE Trans. on Inf. Theory*, vol. IT-44, pp. 1453–1467, July 1998.

[5] B.M. Hochwald and W. Sweldens, "Differential Unitary Space–Time Modulation," *IEEE Trans. on Commun.*, vol. COM-48, pp. 2041–2052, Dec. 2000.

[6] B.L. Hughes, "Differential Space–Time Modulation," *IEEE Trans. on Inf. Theory*, vol. IT-46, pp. 2567–2578, Nov. 2000.

[7] V. Tarokh and H. Jafarkhani, "A Differential Detection Scheme for Transmit Diversity," *IEEE Journal on Selected Areas in Communications*, vol. SAC-18, pp. 1168–1174, July 2000.

[8] R. Schober and L. Lampe, "Noncoherent Receivers for Differential Space–Time Modulation," *Accepted for publication in IEEE Trans. on Commun.*, Nov. 2001.

[9] Y.E. Dallal and S. Shamai (Shitz), "Time Diversity in DPSK Noisy Phase Channels," *IEEE Trans. on Commun.*, vol. COM-40, pp. 1703–1715, Nov. 1992.

[10] C.-D. Chung, "Diversity Coding Technique for Differential Phase Modulation in a Correlated Rayleigh Fading Channel," in *Proceedings of IEEE International Symposium on Personal, Indoor and Mobile Radio Communication (PIMRC)*, London, Sept. 2000, pp. 232–236.

[11] J. Ventura-Traveset, G. Caire, E. Biglieri, and G. Taricco, "Impact of Diversity Reception on Fading Channels with Coded Modulation–Part I: Coherent Detection," *IEEE Trans. on Commun.*, vol. COM-45, pp. 563–572, May 1997.

[12] M. Stojanovic and Z. Zvonar, "Differential Coherent Diversity Combining Techniques for DPSK Over Fast Rayleigh Fading Channels," *IEEE Trans. on Veh. Tech.*, vol. VT-49, pp. 1928–1933, Sept. 2000.

[13] T.-A. Chen, M.P. Fitz, W.-Y. Kuo, M.D. Zoltowski, and J.H. Grimm, "A Space–Time Model for Frequency Nonselective Rayleigh Fading Channels with Application to Space–Time Modems," *IEEE Journal on Sel. Areas in Commun. (JSAC): Wireless Communications Series*, vol. 18, pp. 1175–1189, July 2000.

[14] Ed. W. C. Jakes, Jr., *Microwave Mobile Communications*, Prentice–Hall, New Jersey, 1974.

[15] R. Schober and L. Lampe, "Differential Modulation Diversity," *In Revision: IEEE Trans. on Veh. Tech.*, Mar. 2001.

[16] S. Haykin, *Adaptive Filter Theory*, Prentice-Hall, Upper Saddle River, New Jersey, Third Edition, 1996.

[17] R.J. Young and J.H. Lodge, "Detection of CPM Signals in Fast Rayleigh Flat–Fading Using Adaptive Channel Estimation," *IEEE Trans. on Veh. Tech.*, vol. 44, pp. 338–347, May 1995.

[18] R. Schober and W. H. Gerstacker, "Decision–Feedback Differential Detection Based on Linear Prediction for MDPSK Signals Transmitted Over Ricean Fading Channels," *IEEE Journal on Sel. Areas in Commun. (JSAC)*, vol. 18, pp. 391–402, Mar. 2000.

[19] F. Edbauer, "Bit Error Rate of Binary and Quaternary DPSK Signals with Multiple Differential Feedback Detection," *IEEE Trans. on Commun.*, vol. COM-40, pp. 457–460, Mar. 1992.

[20] M. Schwartz, W. Bennett, and S. Stein, *Communication Systems and Techniques*, McGraw–Hill, New York, 1966.

[21] J.K. Cavers and P. Ho, "Analysis of the Error Performance of Trellis–Coded Modulations in Rayleigh–Fading Channels," *IEEE Trans. on Commun.*, vol. COM-40, pp. 74–83, Jan. 1992.

[22] E. Biglieri, G. Caire, G. Taricco, and J. Ventura-Traveset, "Computing Error Probabilities over Fading Channels: A Unified Approach," *European Transactions on Telecommunications*, vol. 9, pp. 15–25, January-Feburary 1998.

[23] B.M. Hochwald and T.L. Marzetta, "Unitary Space–Time Modulation for Multiple–Antenna Communications in Rayleigh Flat Fading," *IEEE Trans. on Inf. Theory*, vol. IT-46, pp. 543–564, Mar. 2000.

[24] R. Schober, W. H. Gerstacker, and J. B. Huber, "Decision–Feedback Differential Detection of MDPSK for Flat Rayleigh Fading Channels," *IEEE Trans. on Commun.*, vol. COM-47, pp. 1025–1035, July 1999.